Article

Journal of
Nanoscience and Nanotechnology
Vol. 19, 7591–7595, 2019
www.aspbs.com/jnn

Single-Walled Carbon Nanotubes (SWCNTs) and Poly(3,4-ethylenedioxythiophene) Nanocomposite Microwire-Based Electronic Biosensor Fabricated by Microlithography and Layer-by-Layer Nanoassembly

Renyuan Yang[1, †], Zhongcheng Gong[2, †], Xingcai Zhang[3], and Long Que[1, *]

[1] *Department of Electrical and Computer Engineering, Iowa State University, Iowa, 50011, USA*
[2] *Skyworks Solutions, Inc., 01801, USA*
[3] *John A. Paulson School of Engineering and Applied Sciences, Harvard University, Massachusetts, 02138, USA*

Cost-effective single-walled carbon nanotubes (SWCNTs) and poly(3,4-ethylenedioxythiophene) nanocomposite-microwire (N-MWs) electronic biosensor was fabricated by microlithography and layer-by-layer nanoassembly. Using N-MWs, we not only can achieve accurate large-scale registration and integration of nanoscale materials into a functional device, but also can enhance the sensing surface area significantly, which can open great opportunities for the cost-effectively fabrication of ultrasensitive biosensors. Using the binding assay between Protein A and Rabbit Immunoglobulin G (IgG) as a model, measurements find that the N-MWs electronic biosensor, containing carbon nanotubes (CNTs) and conductive polymers, exhibits field effect and the resistance changes upon its binding to biomolecules. The effect of the dimensions of the N-MWs on the sensitivity of the sensor has also been evaluated.

Keywords: Electronic Biosensor, Nanocomposite, Microwire, Layer-by-Layer Nanoassembly, Microlithography.

1. INTRODUCTION

Easy-to-use, cost-effective and ultrasensitive sensors are required for a variety of applications in biological, life science and medical research, security, temperature and infrared sensing, and environment monitoring.[1–9] The sensitivity and selectivity of all types of sensors are essentially determined by the sensing materials. For the past decades, a great deal of nanoscale materials such as carbon nanotubes (CNTs), nanowires (NWs), nanopores and nanoparticles (NPs) have been discovered or synthesized and have shown great potential as advanced sensing materials, offering super sensitivity otherwise impossible by other materials.[10–17] As a result, extensive research efforts have been devoted to develop sensors based on one dimensional (1-D) materials such as single silicon NWs and single CNTs,[10–12] showing great promise for rapid, ultrasensitive biodetection.

However, 1-D materials and related devices using either the bottom-up or the top-down fabrication approaches suffer from some limitations. The bottom-up approach has limitations such as device-to-device uniformity, challenges of large-scale accurate registration and integration of NWs or CNTs. The top-down approach has issues such as expensive and time-consuming fabrication process (e.g., e-beam nanolithography), even though it offers great reliability and scalability to produce uniform and well-aligned Si NWs.[11]

Nanocomposite materials might be one of the options to avoid the aforementioned issues to fabricate functional devices, while still maintaining some unique properties of single NWs or CNTs such as high surface-to-volume ratio and extreme sensitivity for sensing applications. Nanocomposite materials have been evaluated for sensing applications.[18–19] However, how to fabricate ultrasensitive nanocomposite-microwire electronic biosensors is still a challenging endeavour. The layer-by-layer nanoassembly is a facile cost-effective self-assembly method for nanocomposite fabrication, allowing the deposition of

*Author to whom correspondence should be addressed.
†These two authors contributed equally to this work.

materials one layer at a time, with precise nanoscale thickness and abundant choices of material source.[20–24] In this paper, we report a type of electronic microbiosensors based on nanocomposite-microwires (N-MWs) fabricated by combining microlithography and layer-by-layer self-assembly technology.[20–24] The combination of the conventional microlithography method and the versatile layer-by-layer self-assembly technology allows us to fabricate high performance nanocomposite-microwire (N-MWs) electronic biosensor in a facile, cost-effective way.

2. MATERIALS AND METHODS

2.1. Chemicals and Materials

Poly diallyldimethylammonium chloride (PDDA) and poly(3-4-ethylenedioxythiopene)-poly(styrenesulfonate) (PEDOT:PSS) are the polycations while poly(sodium 4-styrenesulfonate) (PSS) is the polyanion. PDDA (409014, Average Mw 1,00,000–2,00,000) and PSS (243051, average Mw 70,000) both were purchased from Sigma. PEDOT:PSS was also purchased from Sigma (483095) in a form of 1.3 wt% dispersion in H_2O. PEDOT constitutes 0.5 wt% while PSS constitutes the remaining 0.8 wt% of the dispersion. This conjugation of the polymers has a conductivity of 1 S/cm. Single-walled carbon nanotubes were purchased from Carbon Solutions Inc. (AP-SWNT). A suspension of these in deionized (DI) water was prepared by sonication for a period of 13 hours. The concentration of nanotubes in the suspension was 25 μg/ml.

Recombinant Protein A produced in *E. coli* was purchased from Thermo Scientific. Protein A binds specifically to the Fc region of the rabbit IgGs. The isoelectric point of protein A is 4.7. Rabbit IgGs used for the experiments were purchased from Sigma. The isoelectric point for the IgGs lies between 5.8 and 7.3. The working concentrations of both protein A and IgG solutions were 1 mg/ml prepared in phosphate buffer. Blocking buffer SEA BLOCK (SB) was purchased from Thermo Scientific and used to prevent direct binding of the IgGs to the sensor surface, which may give rise to false positive signals. Phosphate buffer (1×) of pH 7.5 was purchased form TEKnova and was used to prepare all the solutions. SB solution was prepared by taking one part of the SB against four parts of the phosphate buffer.

2.2. Operational Principle of the Electronic Biosensor

Schematic of a proposed biosensor is shown in Figure 1(a). The sensing element inside each sensor is the nanocomposite-microwire (N-MW), which contains single-walled CNTs (SWCNTs) and poly(3,4-ethylenedioxythiophene) (PEDOT). While CNTs have both metallic and semiconducting components, PEDOT is conductive polymeric materials. The biological samples are delivered to the sensing element through the PDMS microfluidic channels as shown in the figure. Each sensor can be used to monitor one specific biomolecule. Arrayed sensors, which can be easily batch-fabricated on a single chip, therefore, can provide multiplexed biosensing capability.

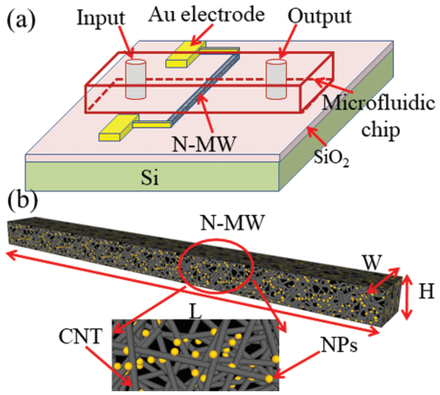

Figure 1. (a) Sketch of a single-walled carbon nanotubes (SWCNTs) and poly(3,4-ethylenedioxythiophene) N-MW based electronic biosensor with PDMS microfluidic channel for sample delivery; (b) sketch of an N-MW ($L \times W \times H$) and its close up showing internal CNTs and NPs.

Assuming the microwire (MW) is a rectangular solid (Fig. 1(b)) with 20 μm (width) × 0.2 μm (height) and 50 μm (length), it can contain hundreds of thousands of 1-D CNTs, 1-D NWs or NPs. As a result, for a MW with the same length of a single NW or a single CNT, it offers (i) the surface area for the binding of biomolecules at least two orders of magnitude larger than that of a single Si NW or CNT; (ii) the sensitivity (e.g., detection of biosamples) at least two orders of magnitude higher than that of a single NW or CNT-based biosensor. In addition, the N-MW based biosensor has the following advantages that are unavailable for a single Si NW and CNT based biosensors: (i) its simplicity and easiness for large-scale integration; (ii) its low cost due to the inexpensive fabrication process by combining optical lithography and layer-by-layer (LbL) nanoassembly technique.[20–24]

2.3. Fabrication of the Nanocomposite Biosensor

The detailed fabrication process flow is illustrated in Figure 2, which involves two major steps: fabrication of N-MWs by combining optical microlithography and LbL nanoassembly process and integration of them within a

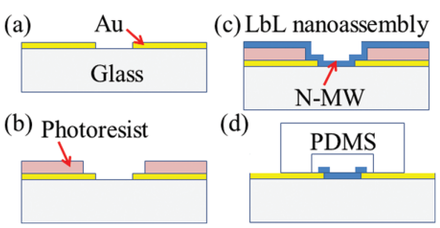

Figure 2. Fabrication process flow of the N-MW based biosensor.

microfluidic chip. Specifically, a silicon dioxide (SiO_2) layer of 500 nm is grown on a silicon substrate. Using a lift-off process, the Au electrodes are patterned. Then the molds for N-MWs synthesis are formed in the photoresist. Thereafter, the wafer is alternately immersed in aqueous poly(dimethyldiallyl ammonium chloride) (PDDA, MW 200 000, Sigma) and sodium poly(styrenesulfonate) (PSS, MW 70 000, Sigma) at a concentration of 3 mg/mL and pH 8, in a sequence of [PDDA (10 min)+PSS (10 min)]$_3$. The subscript 3 refers to the number of immersion of the wafer into the PDDA and PSS solutions, respectively. Between immersions, there is an intermediate rinsing by deionized water for 1 min followed by drying the wafer using a nitrogen gun. These six layers of polyion films enhance the subsequent nanomaterial adsorption in that they form a uniform and strongly charged precursor. Thereafter, PEDOT (Sigma) and SWCNTs (Carbon Solutions, Inc.), taken at 25 μg/mL and pH 8 water dispersion, are added on the precursor layers in the sequence [PDDA (10 min)+PEDOT (10 min)+PDDA (10 min)+SWCNT (20 min)]$_{15}$. The photoresist mold is then removed by acetone and the N-MWs are formed. A polydimethylsiloxane (PDMS) microfluidic channel fabricated separately using a soft-lithography process. Finally, the PDMS microfluidic chip is bonded to the N-MW chip. Note that this method basically can fabricate N-MWs containing any type of nanoscale materials with minimum changes in the process sequences. Hence, it is a simple, inexpensive process of great flexibility.

3. RESULTS AND DISCUSSION

An optical micrograph and a SEM image of an N-MW are given in Figure 3(a). The N-MW consists of the CNTs, PDDA, PSS, and PEDOT with a thickness of 200 nm. A photo of 4 arrayed N-MW based biosensors is shown in Figure 3(b) with an integrated PDMS-based microfluidic interface for biological sample delivery. The N-MW is 70 μm wide and 200 nm thick. Its total length is 1.3 mm and the length for biosensing is 500 μm, which is inside the microfluidic channel.

The operational principle of the N-MW biosensor as shown in Figure 4(a) is similar to that of a single semiconducting NWs and CNTs.[10–12] The electronic transducing signal is the resistance/conductance of the N-MW, which changes when the charged biomolecules are attached to or in close proximity to it due to field effect. Specifically, binding of charged biomolecules with each single CNTs or single nanoparticles within the N-NWs causes the depletion or accumulation of carriers inside CNTs or nanoparticles. As a result, the resistance/conductance of the nanoscale materials changes, so does the N-MWs. It should be noted that theoretically the materials inside the N-MWs can be any kinds of nanoscale materials as far as they are of field effect electrical properties.

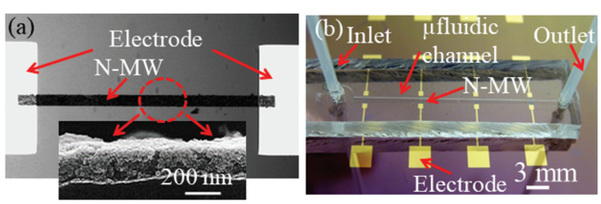

Figure 3. (a) Optical micrograph of a fabricated single-walled carbon nanotubes (SWCNTs) and poly(3,4-ethylenedioxythiophene) N-MW and its corresponding SEM image; (b) a photo of 4 totally assembled N-MW based electronic biosensors.

A protein–protein binding assay is used to demonstrate the operation and biomolecular detection capability of the N-MW sensors. Specifically, the bioassay of the binding between Protein A, which is immobilized on N-MW, and Rabbit Immunoglobulin G (IgG) is performed. As aforementioned, the blocking buffer SB is used to occupy locations of an N-MW without immobilized Protein A to avoid any non-specific binding between Rabbit IgG and the N-MW. To this end, control experiments have been performed and the normalized real-time resistance changes are shown in Figure 4(b). In this case, SB, diluted with phosphate buffered saline (PBS) solution at ratio of 1:4, is first applied on the N-MW, while the measurement is taken every 1 minute. The resistance increases and eventually saturates since SB is gradually immobilized on and occupy all available sites of the N-MW. The PBS solution is then used to rinse the sensor to remove unbound or loosely bound SB, and simultaneously the measurements are taken every 1 minute until the resistance becomes saturated. Thereafter, the rabbit IgG solution with concentration of 1 mg/ml is applied and then PBS solution is again used to rinse the sensor. The measurements are taken as the same as that in the step of applying SB on the N-MW. It is found that the resistance remains essentially unchanged after rabbit IgG is applied, which indicates SB can efficiently block non-specific binding between rabbit IgG with the N-MW. All the measurements are carried out using a HR2 meter (AlphaLab, Inc.), which can measure resistance up to 1.9999 Tera ohms with an accuracy of $\pm$2% for each reading.

The detailed experimental procedure for binding process between Protein A and rabbit IgG is as the following: Firstly, the resistance of the sensor without any biological samples is measured. Secondly, the Protein A solution is applied, while the measurement continues to be taken every 1 minute until the resistance becomes saturated. Thirdly, PBS solution is then used to rinse the sensor to remove unbound or loosely bound Protein A, again the measurements are taken every 1 minute. Fourthly, the measurements are repeated in the same manner as that in the second and third step after Sea Block solution is applied and PBS solution is used to rinse the sensor thoroughly. Finally, the rabbit IgG solution is applied and then PBS

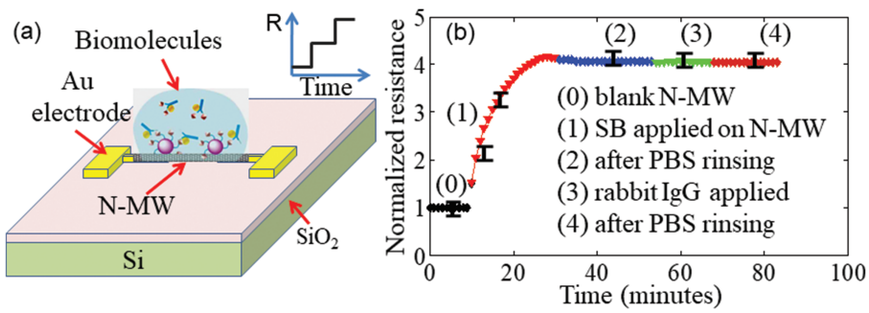

Figure 4. (a) Operational principle of the biosensor: The electronic transducing signal is the resistance of the N-MW, which changes upon the binding of biomolecules with N-MW; (b) control experiment showing the SB can avoid non-specific binding between rabbit IgG and the N-MW.

solution is again used to rinse the sensor. The same measurement procedures are carried out. It should be noted that measurements have been taken continuously before and after the sensors have dried.

In these experiments, the concentrations of Protein A and Rabbit IgG are both at 0.5 mg/ml. Sea Block is diluted with PBS solution at a ratio of 1:4. As shown in the inset in Figure 5, the measured resistance shows a clear change from 8 MΩ for the blank N-MW to 24 MΩ with immobilized Protein A, to 32 MΩ after SB is applied on the sensor and to 38.4 MΩ after the binding between Protein A and rabbit IgG. Real-time monitoring of resistance change of the sensor during this bioassay process is also shown in Figure 5. The staircase change of the resistance of the sensor is clearly observed after sufficient incubation time for each bioassay step. Between each saturated resistance, the resistance is changing gradually, which means the immobilization of biomolecules (e.g., Protein A and SB) on the N-MW is a dynamic process, so is the binding between Protein A and rabbit IgG. It is very clear that the field effect of the CNTs plays an important role in the resistance change of these sensors. However, different from the single CNT or single NW based devices, the resistance change of these sensors is an average effect of the nanomaterials inside the N-MW.

In order to evaluate the effect of the width of N-MW (while the thickness of N-MW is kept the same at 200 nm)

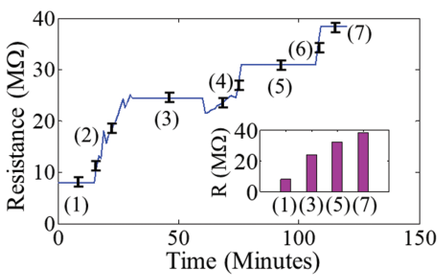

Figure 5. Real-time monitoring of the resistance changes of the N-MW during the bioassay experiments: (1) blank N-MW, (2) Protein A applied, (3) after PBS rinsing, (4) SB applied, (5) after PBS rinsing, (6) rabbit IgG applied, (7) after PBS rinsing. Inset is the measured resistance at step (1), (3), (5) to (7).

of the sensor on the transducing signals, three types of sensors with N-MW widths of 20 μm (Device#1), 30 μm (Device#2) and 70 μm (Device#3) have been fabricated, respectively. With the change in the width of N-MW in the sensors, the total sensing *surface area* exposed to the samples also changes, which means that the total surface area available for the biomolecules to bind to changes. As shown previously, the resistance of the N-NW is influenced by the charges present on the biomolecules. The change in the resistance of the N-MW is the parameter observed to determine the presence of the biomolecules in the test samples. Due to the change in the surface area of the N-MW, the maximum possible number of the charged biomolecules influencing the resistance also changes. In other words, the sensitivity of the sensors is expected to be dependent on the surface area of the sensing components.

In addition, another important parameter to affect the sensitivity is the Debye length of the sensor. Debye length is defined as the length or the distance from the sensing area within which the external charges can have an effect on the mobility of the carriers within the sensing surface.[12, 25]

The percentage change in the resistance (response) of the three sensors for each step is summarized in Figure 6. The sensors show a very good response to the adhesion or presence of protein A. A big percentage change (∼205% to ∼364%) in the resistance can be observed during the procedure to immobilize protein A on these sensors (Fig. 6(a)). In contrast, the sensors show a comparatively very low response (∼0.3% to ∼27%) to the addition of the SB (Fig. 6(b)). This indicates that the occupancy of the binding sites by protein A leaves very few spaces for the SB to bind to. This is why a smaller response is observed during this step (Fig. 6(b)). Note that at this stage, both Protein A and SB adhere directly to the surface of the M-MW. When the IgGs are applied and bind to Protein A through their Fc regions, the resistance of the N-MW changes due to the "Debye effect" since IgGs do not directly bind to the surface of the N-MW. As shown in Figure 6(c), the response of the sensor increases for the sensor with an increased width (from Device#1 to Device#3), suggesting the increased available binding

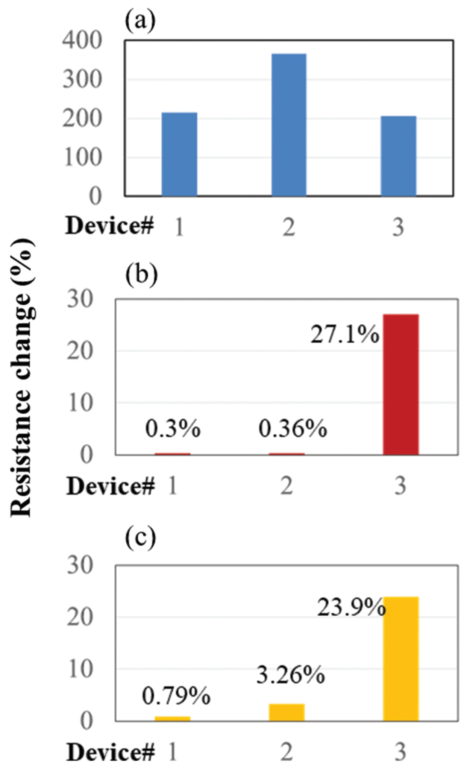

Figure 6. The measured resistance change (%) of sensors with different widths of N-MW at different steps: (a) After being functionalized with Protein A; (b) after being coated with SB; and (c) after being applied IgG. The three sensors have the same thickness of 100 nm and the same length of 500 μm, but have different widths. Device#1: $W_1 = 20$ μm, Device#2: $W_2 = 30$ μm, and Device#3: $W_3 = 70$ μm.

sites for IgGs and thus the change of resistance increases. Based on these experiments, it is evident that Device#3 offers higher sensitivity to detect the molecules (IgGs) in the binding assay. For the Device#3, at the current stage, it has been found as low as 50 μg/ml of IgGs can be detected.

4. CONCLUSIONS

In summary, cost-effective single-walled carbon nanotubes (SWCNTs) and poly(3,4-ethylenedioxythiophene) nanocomposite-microwire electronic biosensors have been fabricated by microlithography and layer-by-layer technology. The combination of optical microlithography and LbL nanoassembly process paves the way for the simple, flexible and rapid fabrication of prototype cost-effective ultrasensitive sensors. As a technical demonstration, the N-MW based electronic biosensors have been used to monitor the binding between Protein A and Rabbit IgG successfully, showing clear resistance changes at each bioassay step. The sensitivity of this type of sensor is dependent on the dimensions of the N-MW. It is anticipated that this type of sensors can be used to detect a variety of biomolecules such as disease biomarkers.

Acknowledgments: The research was funded in part by NSF ECCS 0845370.

References and Notes

1. S. K. Roy, V. T. Sauer, J. N. Westwood-Bachman, A. Venkatasubramanian, and W. K. Hiebert, *Science* 360, eaar5220 (**2018**).
2. E. W. Visser, J. Yan, L. J. van IJzendoorn, and M. W. Prins, *Nature Communications* 9, 2541 (**2018**).
3. L. Jin, J. Li, L. Liu, Z. Wang, and X. Zhang, *Applied Nanoscience* 8, 1189 (**2018**).
4. S. Feng, C. Chen, W. Wang, and L. Que, *Biosens. Bioelectron.* 105, 36 (**2018**).
5. X. Che, Y. He, H. Yin, and L. Que, *Biosens. Bioelectron.* 72, 255 (**2015**).
6. C. Song, P. Deng, and L. Que, *Nanomedicine: Nanotechnology, Biology and Medicine* 14, 1845 (**2018**).
7. H. Jiang (ed.), Optical MEMS for Chemical Analysis and Biomedicine, Institution of Engineering and Technology (IET), Michael Faraday House, Stevenage, UK (**2016**).
8. Y. Tseng, Y. He, S. Lakshmanan, C. Yang, W. Chen, and L. Que, *Nanotechnology* 23, 455708 (**2012**).
9. Y. Tseng, Y. He, and L. Que, *Analyst* 138, 3053 (**2013**).
10. G. Zheng, F. Patolsky, Y. Cui, W. U. Wang, and C. M. Lieber, *Nat. Biotechnol.* 23, 1294 (**2005**).
11. Z. Gao, A. Agarwal, A. D. Trigg, N. Singh, C. Fang, C. Tung, Y. Fan, K. D. Buddharaju, and J. Kong, *Analytical Chemistry*, 79, 3291 (**2007**).
12. K. Maehashi, T. Katsura, K. Kerman, Y. Takamura, K. Matsumoto, and E. Tamiya, *Analytical Chemistry* 79, 782 (**2007**).
13. S. Alzghoul, M. Hailat, S. Zivanovic, L. Que, and G. V. Shah, *Biosens. Bioelectron.* 77, 491 (**2016**).
14. T. Zhang, Y. He, J. Wei, and L. Que, *Biosens. Bioelectron.* 38, 382 (**2012**).
15. P. Pathak and L. Que, *J. Nanosci. Nanotechnol.* 15, 9689 (**2015**).
16. Z. Gong, S. Karandikar, X. Zhang, V. Kotipalli, Y. Lvov, and L. Que, Composite nanomaterial thin film-based biosensors, *IEEE Sensors 2010 Conference* (**2010**), pp. 29–32.
17. P. H. Yeh, Z. Li, and Z. L. Wang, *Adv. Mater.* 21, 4975 (**2009**).
18. C. Jiang, S. Markutsya, Y. Pikus, and V. V. Tsukruk, *Nat. Mater.* 3, 721 (**2004**).
19. P. Dallas, V. K. Sharma, and R. Zboril, *Adv. Colloid Interface Sci.* 166, 119 (**2011**).
20. K. Kang, K. Lee, Y. Han, H. Gao, S. Xie, D. A. Muller, and J. Park, *Nature* 550, 229 (**2017**).
21. G. Decher, *Science* 277, 1232 (**1997**).
22. C. Song, X. Che, and L. Que, *Opt. Express* 25, 19391 (**2017**).
23. Z. Zheng, X. Zhang, D. Carbo, C. Clark, C. A. Nathan, and Y. Lvov, *Langmuir* 26, 7679 (**2010**).
24. G. Parekh, Y. Shi, J. Zheng, X. Zhang, and S. Leporatti, *Therapeutic Delivery* 9, 451 (**2018**).
25. K. Besteman, J. O. Lee, F. G. Wiertz, H. A. Heering, and C. Dekker, *Nano Lett.* 3, 727 (**2003**).

Received: 4 August 2018. Accepted: 26 November 2018.